Carboxylate-alumoxanes as precursors for alumina coatings to enhance the cyclability of LiCoO$_2$

George Ting-Kuo Fey [a,*], Jian-Ging Chen [a], T. Prem Kumar [b]

[a] *Department of Chemical and Materials Engineering, National Central University, Chung-Li, Taiwan 32054, ROC*
[b] *Central Electrochemical Research Institute, Karaikudi 630 006, Tamil Nadu, India*

Abstract

LiCoO$_2$ cathodes coated with Al$_2$O$_3$ derived from carboxylate-alumoxanes have been shown to possess improved cyclability. The carboxylate-alumoxanes were prepared by reacting pseudo-boehmite with acetic and substituted acetic acids. TEM images of the coated powders revealed that the alumina formed a compact kernel of thickness averaging about 20 nm. XRD data on the coated materials suggested the formation of solid solutions of the composition LiAl$_y$Co$_{1-y}$O$_2$ on the surface, a conclusion attested by ESCA depth profiles. Galvanostatic cycling studies suggested that a coating formed from (methoxyethoxy)acetate-alumoxane enhanced the cyclability 13-fold. The improved cyclability is attributed to suppression of the cycle-limiting phase transitions accompanying the charge–discharge processes. The coating procedure based on carboxylate-alumoxanes is economical and environmentally benign, features attractive for industrial exploitation.
© 2005 Elsevier B.V. All rights reserved.

Keywords: Carboxylate-alumoxanes; Al$_2$O$_3$ coating; Coated LiCoO$_2$; Coated cathodes; Lithium battery; Pseudo-boehmite

1. Introduction

LiCoO$_2$ can reversibly cycle lithium between compositions corresponding to $0.5 < x < 1.0$ in Li$_x$CoO$_2$, which limits the charge density to about 140 mAh g^{-1}. The delithiation of LiCoO$_2$ is accompanied by an anisotropic expansion of the host lattice [1,2]. Thus, repeated cycling causes a structural degradation of the host material [3], leading to large capacity fades. The volume changes are ascribed to crystallographic phase transitions occurring in LiCoO$_2$ during charging and discharging at $x < 0.5$ in Li$_x$CoO$_2$ [3,4]. One of the approaches that have been pursued to improve the cyclability of the cathode is to coat it with a thin layer of oxide materials such as Al$_2$O$_3$ [5–9], TiO$_2$ [7,9] and ZrO$_2$ [7,9]. The improved cycling performance of the coated materials is believed to result from structural stability brought about by substitutional oxides formed on the cathode surface [5,6,10–12], as well as by the suppression of cycle-limiting phase transitions during the intercalation–deintercalation processes by high fracture-tough coating materials [7].

Al$_2$O$_3$ as a coating material to improve the cyclability of LiCoO$_2$ has been investigated by several groups [5–9]. The precursors used by these authors have generally been expensive alkoxides such as aluminum sec-butoxide and aluminum ethylhexanate diisopropoxide, which make the commercial exploitation of the coating process questionable. Furthermore, the green bodies of the coating material are generated by a sol–gel procedure in organic solvents. The release of the solvent and alcoholic by-products (formed by the hydrolysis of the alkoxide) during such coating processes can pose an environmental hazard. In this paper, we present the results of our study on commercial LiCoO$_2$ coated with Al$_2$O$_3$ derived from environmentally benign carboxylate-alumoxanes.

2. Experimental

Carboxylate-alumoxane precursors were prepared according to procedures described by Callender et al. [13]. A commercial sample of pseudo-boehmite, [Al(O)(OH)]$_n$

(Plural SB, average particle size: 45 μm; BET surface area: 250 m^2 g^{-1}), was used. Carboxylate-alumoxanes were prepared by reaction of the pseudo-boehmite with acetic acid (A) [CH$_3$COOH], methoxyacetic acid (MA) [CH$_3$OCH$_2$ COOH], (methoxyethoxy)acetic acid (MEA) [CH$_3$OCH$_2$ CH$_2$OCH$_2$COOH], or [(methoxyethoxy)ethoxy]acetic acid (MEEA) [CH$_3$O(CH$_2$CH$_2$O)$_2$CH$_2$COOH]. The carboxylate-alumoxanes were redispersed in water, and sonicated with a commercial sample of LiCoO$_2$ (Coremax Taiwan Corporation), such that the weight ratio of LiCoO$_2$ to Al$_2$O$_3$ (formed upon calcination) was 99:1. A subsequent evaporation of the water and calcination of the resulting dry mass yielded LiCoO$_2$ coated with Al$_2$O$_3$.

Structural analysis of the bare and the coated samples was carried out by X-ray diffraction (Siemens D-5000, Mac Science MXP18). Microstructures of the coated particles were examined by a JEOL JEM-200FXII transmission electron microscope. Depth profiles of aluminum, cobalt and oxygen in the coated materials were recorded by ESCA (VG Scientific ESCALAB 250).

The samples were coupled with lithium in 2032-type coin cells as described elsewhere [14]. The cells were cycled at 0.2 °C rate (with respect to a theoretical capacity of 274 mAh g^{-1}) between 2.75 and 4.40 V in a multi-channel battery tester (Maccor 4000). Phase transitions occurring during the cycling processes were examined by cyclic voltammetry, as described previously [14]. Cyclic voltammograms were run on a Solartron 1287 Electrochemical Interface at a scan rate of 0.1 mV s^{-1} between 3.0 and 4.4 V.

3. Results and discussion

3.1. X-ray diffraction

Thermolysis of carboxylate-alumoxanes, [Al(O)$_x$(OH)$_y$ (OOCR)$_z$]$_n$, formed by the reaction of pseudo-boehmite with carboxylic acids, yields alumina [15,16]. The nature of the carboxylate-alumoxanes depends on the identity of the carboxylic acid used [13]. Thus, we should expect the characteristics of the alumina product to be dependent on the precursor. In fact, the X-ray diffraction pattern of the thermolysis products showed that the product obtained from the acetate-alumoxane was α-Al$_2$O$_3$, while those from the other carboxylate-alumoxanes were γ-Al$_2$O$_3$.

The X-ray diffraction patterns of the bare LiCoO$_2$ and the various Al$_2$O$_3$-coated LiCoO$_2$ powders conformed to the *R3m* symmetry of the core material. Table 1 shows that the lattice constants *a* and *c* of the coated materials differ from those of the bare cathode material, suggesting that solid solutions of composition LiAl$_y$Co$_{1-y}$O$_2$ could have formed by a reaction of the Al$_2$O$_3$ particles with the core LiCoO$_2$ during the 10 h calcination step. It is noteworthy that Bragg reflections relate only to the first few layers of atoms in the crystal lattice. Therefore, XRD patterns correspond only to the surface and not to the bulk of the particle. The I_{003}/I_{104} inten-

Table 1
XRD data on the bare and Al$_2$O$_3$-coated LiCoO$_2$ samples

Coating precursor	a (Å)	c (Å)	c/a	I_{003}/I_{104}	Unit cell volume (Å^3)	R-factor
Bare LiCoO$_2$	2.830	14.001	4.95	1.86	98.0	0.77
A-alumoxane	2.817	14.104	5.01	1.99	96.9	0.45
MA-alumoxane	2.808	13.885	4.94	1.56	94.8	0.45
MEA-alumoxane	2.808	13.914	4.96	1.22	95.0	0.39
MEEA-alumoxane	2.808	13.899	4.95	1.42	94.9	0.49

sity ratios of all the coated materials (Table 1) were higher than 1, and were generally higher than the ratio for the bare LiCoO$_2$, indicating that the samples had good cation ordering [17]. According to Dahn and coworkers [18,19], the R-factor, defined as the ratio of the intensities of the hexagonal characteristic doublet peaks (0 0 6) and (1 0 2) to the (1 0 1) peak, is an indicator of hexagonal ordering. According to the authors [18,19], the lower the R-factor, the better the hexagonal ordering. While the value of the R-factor for the bare LiCoO$_2$ was 0.77, the R-factors for the materials coated with Al$_2$O$_3$ obtained from A-alumoxane, MA-alumoxane, MEA-alumoxane and MEEA-alumoxane were 0.45, 0.45, 0.39 and 0.49, respectively (Table 1). It can be seen that the R-factor values for the coated samples were smaller than that for the bare sample.

3.2. Transmission electron microscopy

Fig. 1 is a TEM image of LiCoO$_2$ coated with Al$_2$O$_3$ obtained from MEA-alumoxane. The alumina coating can be seen as a uniform and compact kernel (light region) over the LiCoO$_2$ particle (dark region). The average thickness of the kernel can be seen to be around 20 nm.
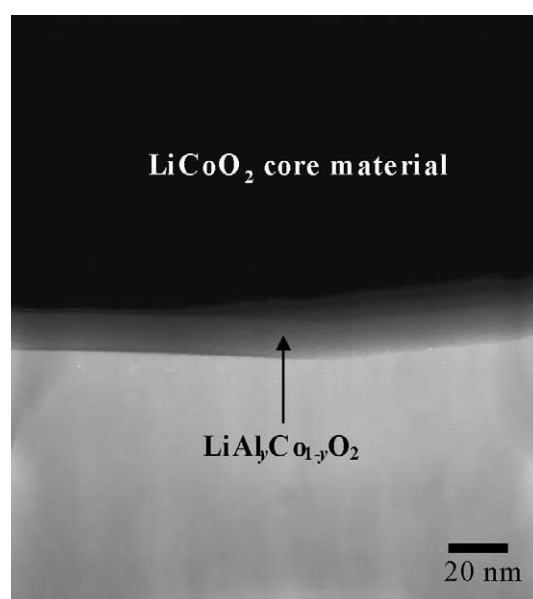

Fig. 1. TEM image of LiCoO$_2$ particle coated with Al$_2$O$_3$ (1.0 wt.%) obtained from MEA-alumoxane.
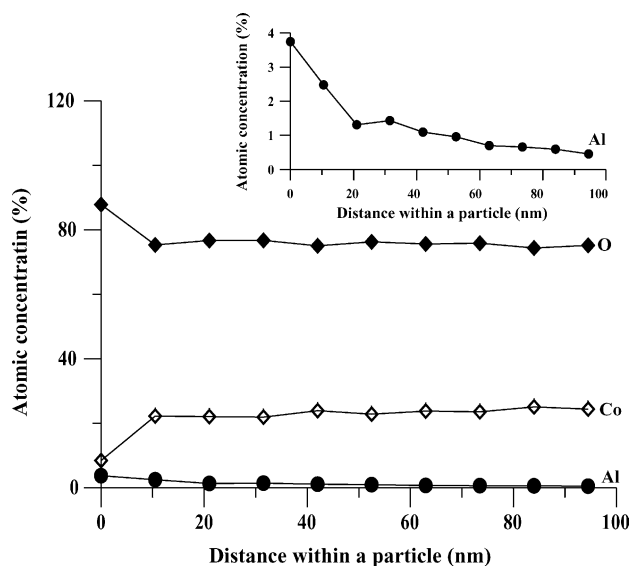
Fig. 2. (a) ESCA depth profiles of $LiCoO_2$ particle coated with Al_2O_3 derived from MEA-alumoxane. (b) Depth profile of aluminum (expanded scale).

3.3. ESCA

The spatial distribution of Al, Co, and O in the alumina-coated $LiCoO_2$ (precursor: MEA-alumoxane) is displayed in the depth profiles presented in Fig. 2. The concentration of cobalt increased to a depth of about 20 nm and then levelled off. The 20 nm depth corresponds approximately to the thickness of the kernel observed with TEM (Fig. 1). The concentration of aluminum was small, typically less than 2 at.% at depths close to 20 nm. Although the Co:Al ratio in the preparation mixture was 1:1, the slightly higher concentration of aluminum vis-à-vis Co on the surface of the coated particle is ascribed to the presence of Al-rich phases (such as Al_2O_3 and $LiAl_yCo_{1-y}O_2$) on the surface. The gradual increase in the cobalt concentration and a simultaneous decrease in the aluminum concentration suggest the formation of substitutional surface oxides, corroborating our XRD results.

3.4. Galvanostatic cycling

The cycling behavior of the various alumina-coated $LiCoO_2$ are compared with that of the bare $LiCoO_2$ in Fig. 3. The first-cycle capacity of the bare $LiCoO_2$ was $168\,\mathrm{mAh\,g^{-1}}$. However, the first-cycle capacities were generally lower for the coated cathodes, being 166, 165, 168 and $166\,\mathrm{mAh\,g^{-1}}$ for $LiCoO_2$ coated with alumina derived from A-alumoxane, MA-alumoxane, MEA-alumoxane, and MEEA-alumoxane, respectively. The lower capacities of the coated materials are attributed to the presence of the electro-inactive alumina and to diminution in the number of Co^{3+} ions available in the substituted surface oxide. The cycling study shows that MEA-alumoxane gave the best results, the $LiCoO_2$ coated with alumina derived from it sustaining 185 cycles before it reached the 80% capacity cut-off based on its
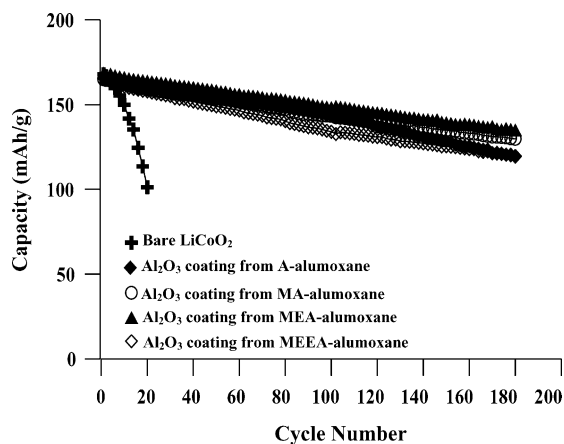

Fig. 3. Cycling behavior of $LiCoO_2$ coated with Al_2O_3 derived from the various carboxylate-alumoxanes.

first-cycle capacity. This is more than a 13-fold improvement in cyclability over the bare sample, which sustained only 14 cycles.

It is expected that because the ratio of the surface area of the alumoxane to its size would decrease as we proceed from the acetate-alumoxane to the higher substituted carboxylate-alumoxanes, the alumina particles formed from the lower order alumoxanes should be closer to one another than those formed from the higher-order alumoxanes. However, the energy released in the thermolysis process, which will be higher for the higher-order alumoxanes, can influence the compactness of the resultant coating and even the particles that comprise it. Furthermore, it must be recalled that the product obtained from the acetate-alumoxane was α-Al_2O_3 while that from the other alumoxanes was γ-Al_2O_3. Thus, the phase of the coating material, its compactness, and the size of the particles that comprise it will determine the effectiveness of the coating.

The cyclability of the materials is generally commensurate with the trend in the variation of the R-factor. Thus, it can be seen from Table 1 that the bare material with an R-factor value of 0.77 sustained only 14 cycles, while the R-factor values of the alumina-coated materials derived from A-alumoxane, MA-alumoxane, MEA-alumoxane and MEEA-alumoxane (and their corresponding cycle-lifes in parentheses) were 0.45 (135), 0.45 (159), 0.39 (185) and 0.49 (110). The cyclability was the maximum for $LiCoO_2$ coated with alumina derived from the MEA-alumoxane.

3.5. Cyclic voltammetry

Cyclic voltammetry is sensitive to phase transformations occurring during electrochemical reactions [20]. A slow-scan cyclic voltammogram recorded with the bare $LiCoO_2$ is presented in Fig. 4a, which shows peaks corresponding to the hexagonal–monoclinic–hexagonal phase transitions. Furthermore, these peaks persisted during repeated cycling. However, the cyclic voltammogram of $LiCoO_2$ coated with
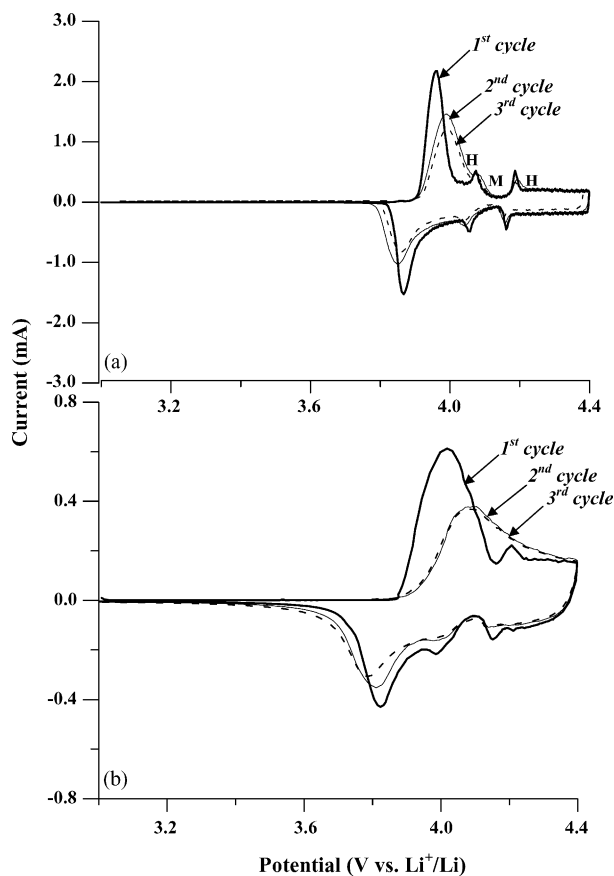
Fig. 4. Cyclic voltammograms of (a) bare LiCoO$_2$ and (b) LiCoO$_2$ coated with Al$_2$O$_3$. Precursor: MEA-alumoxane.

Al$_2$O$_3$ derived from MEA-alumoxane (Fig. 4b) shows that the peaks corresponding to the phase changes appeared only in the first sweep, and that from the second sweep onwards, these peaks were conspicuously missing, suggesting that any defect in the coating that might have been present initially was repaired upon cycling. The presence of cracks, pinholes, and other coating defects on coated surfaces is inevitable. However, such defects may form and close with the application of a load, or upon thermal cycling. In our case, changes in the surface texture that occurred as a result of the contraction and expansion of the lattice during the cycling process may have enabled the particles of the coating material to become ingrained in the crevices and cracks on the cathode surface. The resultant compact kernel led to a suppression of the phase transitions, enhancing the cyclability of the coated material.

4. Conclusions

Carboxylate-alumoxanes were used as precursors for coating commercial LiCoO$_2$ cathode samples with Al$_2$O$_3$. XRD data suggested that upon calcination the coated alumina particles formed a substitutional compound of the type LiAl$_y$Co$_{1-y}$O$_2$ on the surface. TEM images and ESCA depth profiles indicated that a surface layer of average thickness of

about 20 nm was formed on the cathode particles. Cycling studies showed that a 13-fold improvement in the cyclability of LiCoO$_2$ was effected by the coating derived from MEA-alumoxane. The lowest R-factor value of this coated material indicates that good structural stability of the sample contributed to its high cyclability.

In addition to its simplicity, this process employs no hazardous organic solvents, which makes it viable for commercial exploitation. Additionally, it uses commercially available pseudo-boehmite and alkoxy-substituted acetic acids, which present a cost advantage over the expensive alkoxide precursors used in sol–gel coatings. The infinite stability, both as a solid and as an aqueous solution, of the nanoparticulate carboxylate-alumoxane precursors (as compared to moisture-sensitive sol–gel precursors) and the aqueous solution processing are added advantages.

Acknowledgements

References

[1] J.N. Reimers, J.R. Dahn, J. Electrochem. Soc. 139 (1992) 2091.
[2] T. Ohzuku, A. Ueda, J. Electrochem. Soc. 141 (1994) 2972.
[3] H.F. Wang, Y.I. Jang, B.Y. Huang, D.R. Sadoway, Y.M. Chiang, J. Electrochem. Soc. 146 (1999) 473.
[4] S. Lavasseur, M. Menetrier, E. Suard, C. Delmas, Solid State Ionics 128 (2000) 11.
[5] J. Cho, Y.J. Kim, B. Park, Chem. Mater. 12 (2000) 3788.
[6] J. Cho, Y.J. Kim, B. Park, J. Electrochem. Soc. 148 (2001) 1110.
[7] J. Cho, Y.J. Kim, T.-J. Kim, B. Park, Angew. Chem. Int. Ed. 40 (2001) 3367.
[8] L. Liu, Z. Wang, H. Li, L. Chen, X. Huang, Solid State Ionics 152/153 (2002) 341.
[9] A.M. Kannan, L. Rabenberg, A. Manthiram, Electrochem. Solid-State Lett. 6 (2003) 16.
[10] M. Mladenov, R. Stoyanova, E. Zhecheva, S. Vassilev, Electrochem. Commun. 3 (2001) 410.
[11] Z. Wang, C. Wu, L. Liu, F. Wu, L. Chen, X. Huang, J. Electrochem. Soc. 149 (2002) 466.
[12] J. Cho, C.-S. Kim, S.-I. Yoo, Electrochem. Solid-State Lett. 3 (2000) 362.
[13] R.L. Callender, C.J. Harlan, N.M. Shapiro, C.D. Jones, D.L. Callahan, M.R. Wiesner, D.B. MacQueen, R. Cook, A.R. Barron, Chem. Mater. 9 (1997) 2418.
[14] G.T.K. Fey, C.Z. Lu, T. Prem Kumar, J. Power Sources 115 (2003) 332.
[15] R.L. Callender, A.R. Barron, Adv. Mater. 12 (2000) 734.
[16] C.J. Harlan, A. Kareiva, D.B. MacQueen, R. Cook, A.R. Barron, Adv. Mater. 9 (1997) 68.
[17] J. Kim, P. Fulmer, A. Manthiram, Mater. Res. Bull. 34 (1999) 571.
[18] J.N. Reimers, E. Rossen, C.D. Jones, J.R. Dahn, Solid State Ionics 61 (1993) 335.
[19] J.R. Dahn, U. von Sacken, C.A. Michal, Solid State Ionics 44 (1990) 87.
[20] L. Kavan, M. Gratzel, Electrochem. Solid-State Lett. 5 (2002) 39.